Ionospheric post-seismic perturbations following the Tokachi-Oki earthquake from high rate GPS japanese data : wave source and propagation

Crespon, F. (1,2) ; Occhipinti, G. (1) ; Garcia, R. (1) ; Lognonné, P. (1) and Murakami, M. (3)

(1) Institut de Physique du Globe de Paris, Département de Géophysique Spatiale et Planétaire, 4 avenue de Neptune, 94107, St Maur des Fossés, France

(2) Noveltis, Parc Technologique du Canal, 2 rue de l'Europe, 31520, Ramonville, France

(3) Geographical Survey Institute, Geography and Crustal Dynamics Research Center, Kitasato-1, Tsukuba, 305-0811 Japan

Abstract:

Ionospheric perturbations following the Tokachi-Oki earthquake (East of Hokkaido island) have been sensed by the high rate continuous GPS Network of Japan. The strong motions have produced infrasonic waves propagating into the ionosphere and generating electronic density perturbations. The electronic content along GPS satellite to GPS receiver rays is extracted from the raw data. The attenuation of infrasonic waves by the atmosphere is demonstrated on these signals.

Then, the GPS data have been inverted to reconstruct 3D tomographic images of the electronic density perturbations. The ionospheric waves far from the source are propagating horizontally at the speed of seismic surface waves and vertically at the speed of sound in the atmosphere. Close to the source, the signal has been analyzed and modeled in order to constraint the source location and the source mechanism. These studies demonstrate the interest of post-seismic ionospheric perturbations to retrieve the long period strong motions that are not avalaible inland due to the saturation of seismometers, and in the ocean due to the low number of ocean bottom seismometers.

Earth-atmosphere coupling:

The first theories developed to explain waves shock induced by earthquakes have not considered the coupling between the solid Earth and the atmosphere/ionosphere system and were based on the physics of acoustic-gravity waves [Hines, 1960]. A more detailed theory, based on normal modes theory, was then developed by Lognonné et al [1998] and improved by Artru et al. [2001] to take into account the coupling between the solid Earth, the ocean and the atmosphere.

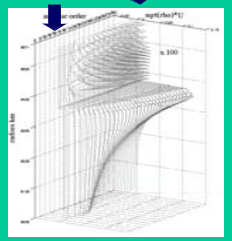

Solid modes n=0, l=2-300

Figure 1: Normal modes for Earth with an atmosphere.

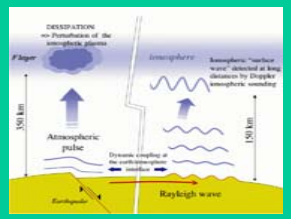

Figure 2: Schematic view of the Earth-atmosphere coupling after an earthquake.

So propagative modes with frequency higher than Vaisala frequency match to acoustic waves that propagate upward to the ionosphere. These waves are generated by vertical ground displacements that appear at near field (rupture process) and at far field (Rayleigh surface waves) as shown on Figure 2.

The Tokachi-Oki earthquake 09/25/2003 Mw8.3:

On 25 September 2003, in the Tokachi_Oki region, a great earthquake occurred at 19:50 (GMT) and was located at 144,1°W and 42,2°N. In this region the Pacific plate subduct beneath the Hokkaido region from the Kurile Trench at a rate of about 80 mm/year and generate large earthquakes since decades (Fig. 3). The earthquake of the 25 September is one of them and induced strong vertical ground motion. The Centroid Moment Tensor (CMT) computed by Havard Seismology Institute and USGS are respectively (FP1: strike=250, dip=11, slip=132 ; FP2: strike=28, dip=82, slip=83) and (FP1: strike=234, slip=7, dip=103 ; FP2: strike=41, dip=83, slip=88).

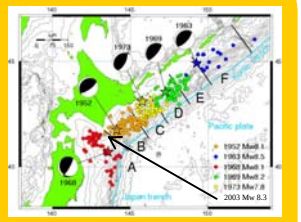

Figure 3: Distribution of great earthquakes by Tomoya HARADA (Department of Earth and Planetary Sciences, Kobe University).

Ionospheric perturbation induced by the Tokachi-Oki earthquake Mw8.3:

For this study we used the Japan network (GEONET) which have environ 1000 GPS stations with a 1s sampling rate (data provided by M. Murakami). The ionospheric perturbations were detected by the satellite PRN13, PRN24 and PRN27. Fig. 5 present the STEC of satellite PRN13 function of time and epicentral range.

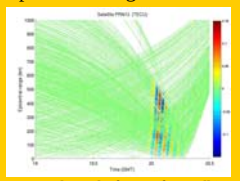

Figure 5: Hodograph of STEC for satelltie PRN13

3D tomography :

So we computed the 3D tomography of these perturbations. Results are presented on Fig. 6 for a vertical cut, with azimuth 45°, in the 3D grid twelve minutes after the earthquake. The arrival time and propagation velocities of the ionospheric perturbations are coherent with expected waves at middle and far field as for others treated earthquakes [Garcia et al., 2005].

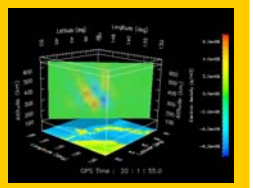

Figure 6: vertical cut in the 3D grid (Red square: epicenter)

These results are in good agreement with theory but we want to use the ionospheric GPS observations to constrain a few parameters of the rupture process. So, using normal modes theory extended to the atmosphere, we developed a model of atmospheric waves generated by earthquakes. The Fig. 7 present the vertical displacement of the atmosphere induced at 250 km altitude a few minutes after the earthquake.

Conclusion:

The atmospheric waves are modeled but we have to link electron density variation to neutral density variation. Then, integrating electron density variations along satellite-receiver ray path, we will be able to produce synthetic GPS data of the modeled ionospheric perturbations in order to do reliable comparisons with GPS observations. Finally we will get a forward model of the generation of ionospheric perturbations induced by earthquake and we foresee to constraint rupture process by inversion.

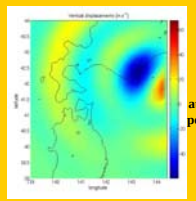

Figure 7: Model of atmospheric perturbation

Reference:

Artru J., P. Lognonné et E. Blanc, Normal modes modeling of post-seismic ionospheric oscillations, *Geophysical Res. Lett.*, **28**, 697-700, 2001.

Hines, C.O., Internal atmospheric gravity waves, *Canadian Journal of Physics*, *38*, 1441-1481, 1960.

Garcia, R., F. Crespon, V.Ducic, P. Lognonné, 3D ionospheric tomography of the Denali seismo-acoustic waves over California, GJI., in press, 2005.

Lognonné, P., C. Clévédé and H. Kanamori, Normal mode summation of seismograms and barograms in an spherical Earth with realistic atmosphere, GJI, **135**, 388-406,1998.

Ionospheric signal in GPS data:

The dispersive effect of the ionosphere on electromagnetic waves allow us to link electron density and data provided by bistatic GPS receivers. Indeed the combinations of pseudo ranges P1 and P2, and phase data L1 and L2 ,respectively at frequency f_1 (1575.42MHz) and f_2 (1227.60MHz), match to the integrated electron density along ray path. This data is usually called Slant Total Electron Content (STEC).

$$STEC = K(\lambda_1 L_1 - \lambda_2 L_2) - \langle(\lambda_1 L_1 - \lambda_2 L_2) + (P1 - P2)\rangle$$

with c: light velocity.

λ_1, λ_2: wavelenghts of frequencies f_1, f_2.

$$K = \frac{c}{40{,}3} \frac{f_2^2 f_1^2}{f_2^2 - f_1^2}$$

The STEC is filtered between 3.8 mHz and 7 mHz in order to detect ionospheric perturbations induced by atmospheric acoustic waves. The Fig. 4 present the mean of power spectral density of STEC.

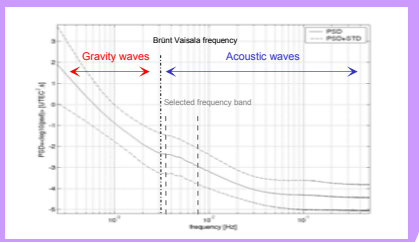

Figure 4: Power spectral density of ionospheric GPS data

3D tomography of ionospheric waves:

Using a 3D grid over a dense network of GPS receivers and modeling the filtered STEC by the integrated local variation of plasma density, we are able to retrieve 3D structure of the ionospheric perturbations [Garcia et al., 2005].

Inverse problem :

- Interpolation operator : $\Delta STEC = \int_{ray(i)} \Delta\rho$.
- LMS method.